

Fracture Mechanics of Concrete Structures
Proceedings FRAMCOS-3
AEDIFICATIO Publishers, D-79104 Freiburg, Germany

MODELLING SPLITTING AND FATIGUE EFFECTS OF BOND

K. Lundgren and K. Gylltoft
Division of Concrete Structures, Chalmers University of Technology
Sweden

Abstract

When deformed bars are anchored in concrete, this causes not only bond stresses, but also splitting stresses that are usually not taken into account in FE-analyses of reinforced concrete structures. Therefore, a model has been developed which takes the three-dimensional splitting effect, and also the effect of cyclic loading and changing slip direction into account. Bar pull-out tests with various geometry and with both monotonic and cyclic loading have been analysed. With the same input parameters, various bond-slip curves were obtained, depending on the modelled geometry and strength of the surrounding concrete. The results show that the new model is capable of predicting splitting failures, and of dealing with cyclic loading in a physical reasonable way.

Key words: Bond, splitting failure, cyclic loading, non-linear fracture mechanics, finite element analyses

1 Introduction

When modelling reinforced concrete structures with the finite element method, it is common to assume either perfect bond between the reinforcement bars and the surrounding concrete, or a bond-slip relation for an interface layer. However, none of these methods take the three-dimensional splitting effect into account, which can be of importance

when for example the concrete cover is insufficient and spalling will occur. Also, the effect of cyclic loading with varying slip direction is important for the bond resistance. Therefore, a model has been developed which takes the three-dimensional splitting effect, and the effect of cyclic loading into account. The model is presented here, together with results from finite element analyses of pull-out tests.

2 Modelling of the interface

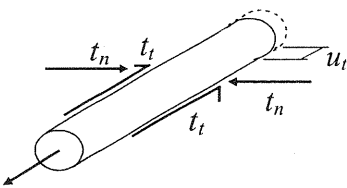
In the finite element program DIANA, there are interface-elements available, which can be used to model the bond-slip behaviour between reinforcement bars and concrete. The element describes a relation between the tractions \mathbf{t} and the relative displacements \mathbf{u} in the interface. The physical interpretation of the variables t_n , t_t , u_n and u_t is shown in Fig. 1.

2.1 Elasto-plastic formulation

Åkesson (1993) has developed a frictional model for anchorage of strands, using elasto-plastic theory to describe the relations between the stresses and deformations to include the splitting effects. The model was intended to be used only for monotonic loading. Therefore, a new model has been developed, still using elasto-plastic theory. The splitting effects are included, and the model is capable of dealing with cyclic loading and varying slip direction. The relation between the tractions \mathbf{t} and the relative displacement \mathbf{u} is in the elastic range:

$$\begin{bmatrix} t_n \\ t_t \end{bmatrix} = \begin{bmatrix} D_{11} & \frac{t_t}{|t_t|} D_{12} \\ 0 & D_{22} \end{bmatrix} \begin{bmatrix} u_n \\ u_t \end{bmatrix} \quad (1)$$

where D_{12} normally is negative, meaning that slip in either direction will cause negative t_n ; i. e. compressive forces directed outwards in the concrete.



t_n = normal stress
 t_t = bond stress
 u_n = relative normal displacement
in the layer (not shown in the figure)
 u_t = slip

Fig. 1 Physical interpretation of the variables t_n , t_t , u_n and u_t .

The model is further equipped with yield lines, flow rules, and hardening laws. The yield lines are two yield functions; one describing the friction F_1 , and one describing the upper limit, a cap F_2 .

$$F_1 = |t_t| + \mu(t_n - t_{n0}) = 0 \quad (2)$$

$$F_2 = |t_t| - t_n - c = 0 \quad (3)$$

For plastic loading along the yield line describing the upper limit, F_2 , an associated flow rule is assumed. For the yield line describing the friction, F_1 , a non-associated flow rule is assumed, where the plastic part of the deformations are

$$d\mathbf{u}^p = d\lambda \frac{\partial G}{\partial \boldsymbol{\alpha}}, \quad G = |t_t| + \eta(t_n - t_{n0}) = 0. \quad (4)$$

The yield lines, together with the direction of the plastic part of the deformations are shown in Fig. 2. At the corners, a combination of the two flow rules is used.

2.2 Damaged / undamaged deformation zones

A typical response for bond with varying slip direction is with a steep unloading and then an almost constant, low bond stress until the original monotonic curve is reached. To make the model describe this typical response, a new concept, called *damaged / undamaged deformation zone*, is used. The idea is that when the reinforcement is slipping in the concrete, the friction will be damaged in the range of the passed plastic slip. As shown in Fig. 3, slipping of the reinforcement in one direction

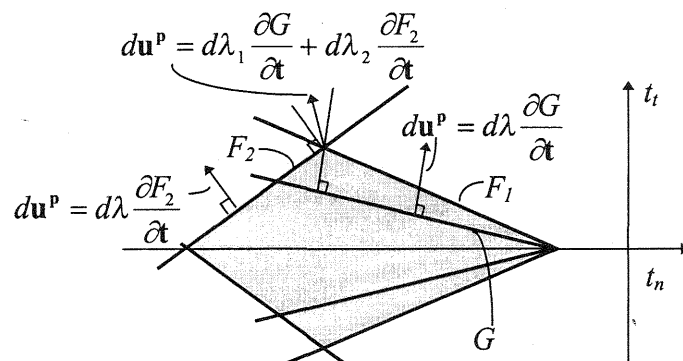


Fig. 2 The yield lines with an associated flow rule at the yield line describing the upper limit, F_2 , and a non-associated flow rule at the yield line describing the friction, F_1 .

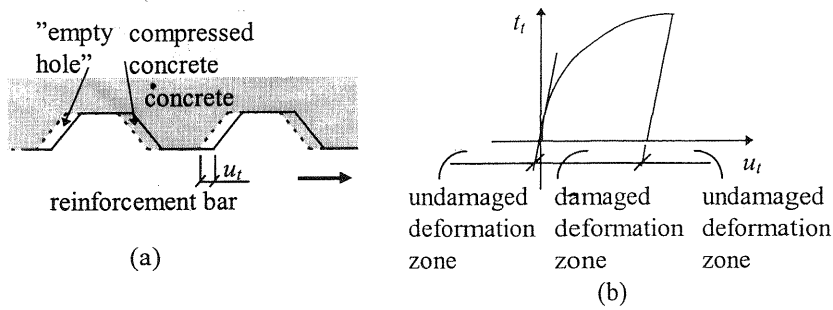


Fig. 3 (a) Slipping of the reinforcement in one direction will theoretically cause compressed concrete in front of the ribs, and "empty holes" behind the ribs; and (b) The range of the slip where plastic deformations have occurred is called the damaged deformation zone.

will theoretically cause compressed concrete in front of the ribs, and "empty holes" behind the ribs. When the loading is reversed, first of all the elastic part of the slip will cause unloading. For further unloading in the damaged deformation zone a low coefficient of friction, μ_d , is assumed until the interface is back in the undamaged deformation zone again. Also the parameter η has a lower value in the damaged deformation zone, η_d , physically corresponding to that the increase in the stresses is lower than in the undamaged deformation zones.

2.3 Hardening

For the hardening rule of the model, a hardening parameter κ is established. It is defined as

$$d\kappa = \sqrt{du_n^{p^2} + du_t^{p^2}} \text{ in the undamaged deformation zones, and} \quad (5)$$

$$d\kappa = \frac{\eta_d}{\eta} \sqrt{du_n^{p^2} + du_t^{p^2}} \text{ in the damaged deformation zones.} \quad (6)$$

It can be noted that for monotonic loading are du_n^p and the elastic part of the slip very small compared to the plastic part of the slip, du_t^p ; therefore the hardening parameter κ will be almost equivalent to the slip, u_t . The variables μ and c in the yield functions are assumed to be functions of κ .

Also, the apex of the yield surface is moved in the direction of the loading, see Fig. 4. This can be compared with a kinematic hardening. However, for further loading in one direction, this movement will have no effect on the yield line. Therefore, the apex is moved partwise when the interface returns to the undamaged deformation zone, after being in the damaged deformation zone. In Fig. 4, an example of how the apex t_{n0} is moved is shown.

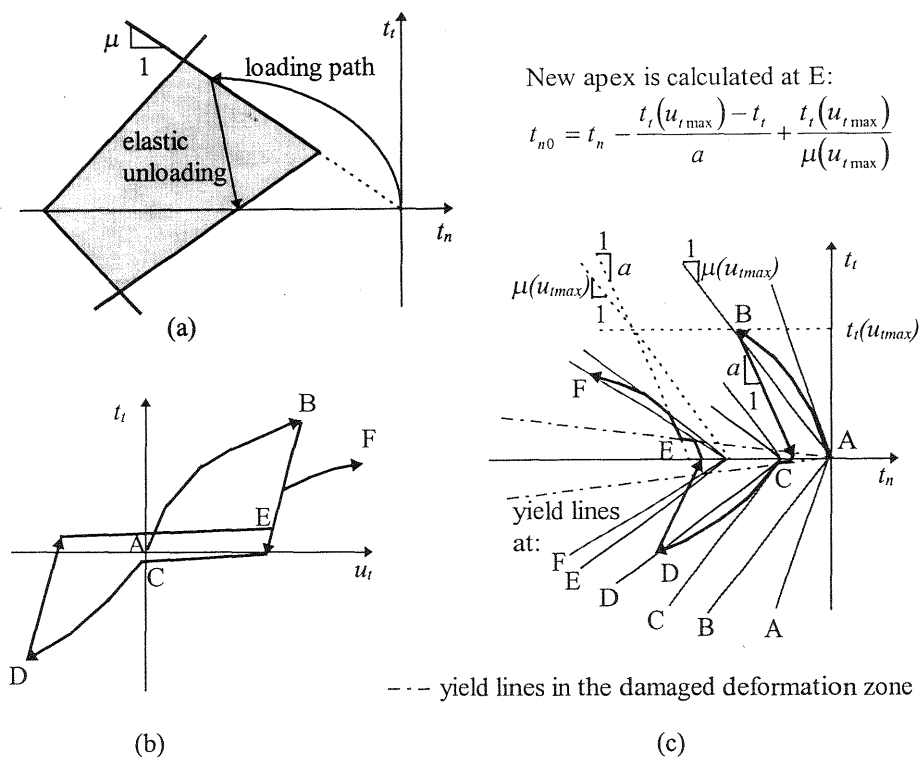


Fig. 4 (a) The apex of the yield lines is moved in the direction of the loading; (b) bond-slip curve; and (c) the corresponding load cycle in the stress space, showing how the apex is moved partwise.

3 Comparison with pull-out tests

The new interface model has been used in FE-analyses to model experiments found in literature. In all analyses, the concrete was modelled with a constitutive model based on non-linear fracture mechanics with a combined Drucker-Prager and Rankine elasto-plastic model. The FE-models were axisymmetric; the localization of the deformations due to cracking of the concrete was then smeared out over the concrete elements assuming that there were four radial cracks in a cylinder. Yielding was modelled using associated flow and isotropic hardening. The hardening of the Drucker-Prager yield surface was evaluated from the shape of the uniaxial stress-strain relationship in compression, and was chosen to match typical test data presented by Kupfer and Gerstle (1973), see Fig. 5b. From the various measured compressive strengths, an equivalent compressive cylinder strength, f_{cc} , was evaluated. Other necessary material data for the concrete was

calculated according to the expressions in CEB (1993) from f_{cc} , and is shown in Table 1. The constitutive behaviour of the reinforcement steel was modelled by the von Mises yield criterion with associated flow and isotropic hardening. The elastic modulus of the reinforcement was assumed to be 200 GPa.

Table 1. Material data of the concrete in the analysed pull-out tests

Reference	Compressive tests		Material data used in the analyses			
	Test specimen	f_{cc} [MPa]	f_{cc} [MPa]	f_{ct} [MPa]	E_c [GPa]	G_F [N/m]
Noghabai	150 mm cube, wet	47.6	35.7	2.7	32.9	73
Magnusson	150 mm cyl., wet	27.5	27.5	2.2	30.0	90
Balázs and Koch	150 mm cube, wet	28-32	25.5	2.0	29.4	58

3.1 Input parameters for the interface

Required input data for the interface is the elastic stiffness matrix \mathbf{D} in equation (1), the initial apex of the yield lines t_{n0} in equation (2), the parameter η defined in equation (4), and for loading in the damaged deformation zone the parameters η_d and μ_d . Furthermore, the functions $\mu(\kappa)$ and $c(\kappa)$ must be chosen.

First of all, the stiffness D_{22} in the elastic stiffness matrix \mathbf{D} is recognized as the stiffness of the first part, or at unloading, in a bond-slip curve. This stiffness was in the tests of Balázs and Koch (1995) about $4 \cdot 10^{11}$ N/m, when the concrete compressive strength was 27.5 MPa. Since this stiffness depends on the concrete quality, it was therefore chosen to:

$$D_{22} = 14.5 \cdot 10^3 f_{cc} \quad (7)$$

Next, the stiffnesses D_{11} and D_{12} were determined. To make the model describe a bond-slip curve with an initial stiffness of about D_{22} , and then decreasing, these parameters were chosen to be:

$$D_{12} = -0.98 \frac{D_{22}}{\mu_{\max}} \quad (8)$$

$$D_{11} = 1.7 \cdot 10^3 f_{cc} \quad (9)$$

The adhesional strength between the reinforcement bar and the concrete was assumed to be negligible; i. e. the initial apex of the yield lines t_{n0} was chosen to be zero. The parameter η is chosen in order to obtain a decreasing bond stress when the concrete around the bar splits, without

elastic unloading. Through calibration, η was chosen to be 0.05. For loading in the damaged deformation zones, η_d was chosen to be $\eta/400$, and the coefficient of friction μ_d was 0.3.

The function $\mu(\kappa)$ describes how the relation between the bond stress and the normal splitting stress depends on the hardening parameter. Tepfers and Olsson (1992) performed “ring tests”; pull-out tests in concrete cylinders confined by thin steel tubes. They measured the strain in the steel ring and used this to evaluate the normal stress. Also in some of the pull-out tests in Noghabai (1995), concrete cylinders were confined by steel tubes, and the measured steel strains have been used to evaluate the splitting stress in Lundgren and Gylltoft (1997). The results, together with the chosen input for the analyses are shown in Fig. 5a.

The variable c represents the upper limit of the stresses t_n and t_t and combinations of them as shown in Fig. 2. This upper limit shall represent the case with a pull-out failure. A theoretical consideration of a case with zero bond stress will then lead to a limit of the normal splitting stress about the compressive strength of the concrete. The function $c(\kappa)$ was therefore chosen to be the same as the uniaxial compression curve of the concrete, only with a factor between the plastic strain and the hardening parameter κ as shown in Fig. 5b.

3.2 Monotonic pull-out tests

Bar pull-out splitting tests performed by Noghabai (1995), Magnusson (1997) and Balázs and Koch (1995) have been analysed. In Noghabai (1995), the test specimens consisted of concrete cylinders with diameter 313 mm, with deformed reinforcement bars, $\phi 32$ mm Ks 400. The embedment length was 120 mm. In two of the three performed tests, the

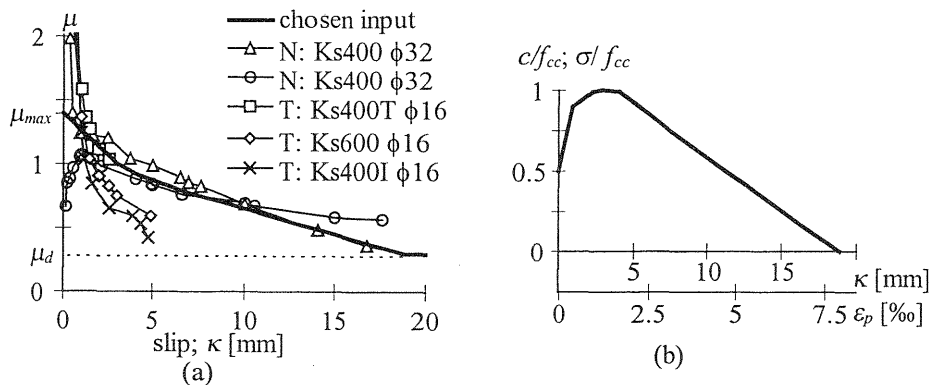


Fig. 5 (a) The coefficient of friction as a function of the slip evaluated from tests, N: Noghabai (1995), T: Tepfers and Olsson (1992), together with the chosen function $\mu(\kappa)$; and (b) Compressive stress versus plastic strain, and the function $c(\kappa)$.

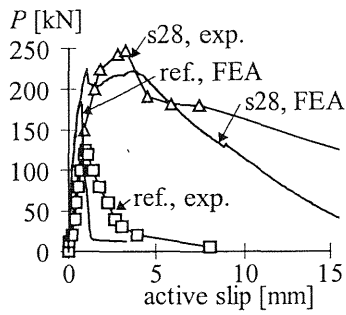
concrete cylinders were reinforced with spiral reinforcement, $\phi 6$ mm Ks 400 with a radius of 40.5 mm, with varying pitches s_{14} and s_{28} mm. This spiral reinforcement was modelled as embedded reinforcement, meaning that complete interaction between the steel and the concrete was assumed. Noghabai (1995) also performed other pull-out tests with the same reinforcement bars, $\phi 32$ mm Ks 400, with concrete cylinders confined by 10 mm thick steel tubes. The diameter of the concrete specimen was 219 mm and the embedment length was 80 mm.

Magnusson (1997) and Balázs and Koch (1995) have performed pull-out tests with deformed reinforcement bars, $\phi 16$ mm K 500. Magnusson had concrete cylinders with a diameter of 300 mm and an embedment length of 40 mm; Balázs and Koch had concrete specimens with a quadratic cross-section $160 \cdot 160$ mm and an embedment length of 80 mm. In both cases, the concrete specimens were large enough to prevent splitting failure; thus, pull-out failures were obtained. To reduce the numerical difficulties, the quadratic cross-section was approximated as axisymmetric.

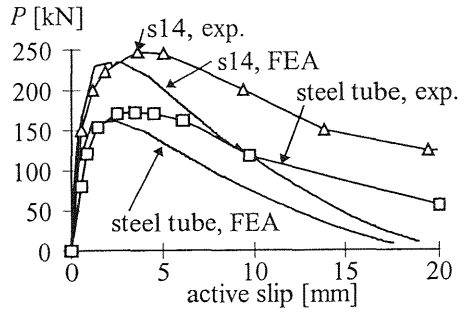
The calculated load versus slip for these tests are shown in Fig. 6, together with results from the experiments. Especially in Fig. 6a it can be seen that even with the same embedment length, and when exactly the same input parameters were given for the interface, different load-slip curves were obtained depending on the modelled structure. Comparing with the measured response, the agreement is rather good, especially when considering the large scatter that is always obtained in pull-out tests. Another important thing to compare is the failure mode, which is correct in all cases; splitting failure in Noghabai's test without spiral reinforcement, a combination when spiral reinforcement with pitch s_{28} mm was used, and pull-out failure in the other cases. In Fig. 6d, the deformed FE-mesh and the tangential stresses at maximum load is shown for Noghabai's test without spiral reinforcement. There it can be seen that the maximum load is obtained when the crack reaches the outer edge. The elements inside this line are already cracked, and the stresses are on the descending branch.

3.3 Cyclic pull-out tests

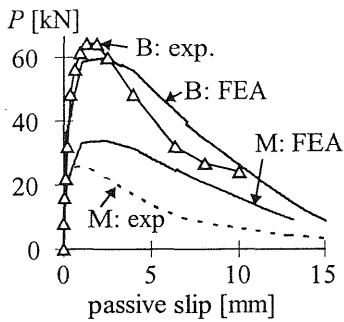
Balázs and Koch (1995) have performed large investigations of pull-out tests loaded with cyclic loading. The test specimens had the same geometry as in their monotonic tests, described in the previous section. One test, with cyclic load varying from -25% to 25% of the maximum load in the monotonic tests have been analysed with the same finite element model as in the monotonic tests, using the new model. Results from the experiments, together with results from the analyses are shown in Fig. 7.



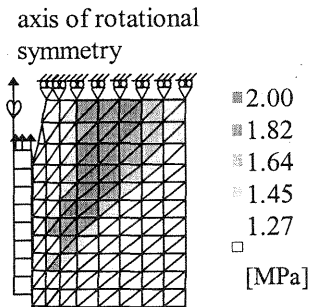
(a) Noghabai (1995)



(b) Noghabai (1995)



(c) B: Balázs and Koch(1995)
M: Magnusson (1997)



(d)

Fig. 6 (a), (b), and (c) Load versus slip in monotonic pull-out-tests; and (d) The deformed FE-mesh and the tangential stresses (in the direction out of the plane) at maximum load in Noghabai's test without spiral reinforcement.

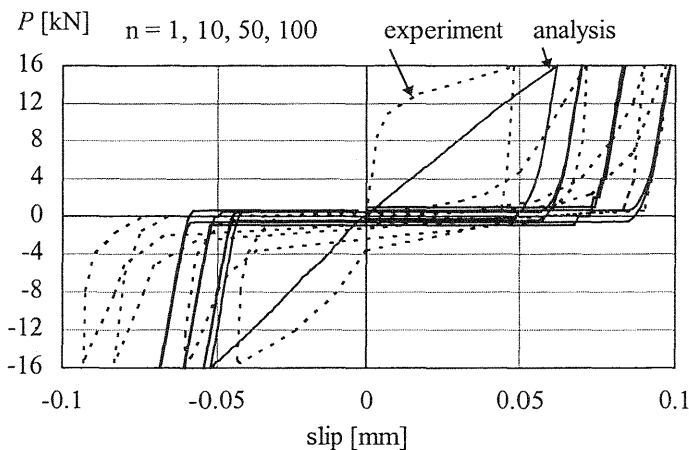


Fig. 7 Load versus slip in cyclic pull-out-tests, Balázs and Koch (1995).

4 Conclusions

A new model describing bond between deformed reinforced bars and concrete has been developed. Since the model takes the three-dimensional splitting effect into account, the same input parameters will result in different load-slip curves depending on the geometry and loading conditions of the concrete specimen. The model can also describe the behaviour in cyclic loading in a realistic way, and reasonable good agreement with experiments was found.

References

- Balázs, G. and Koch, R. (1995) Bond Characteristics Under Reversed Cyclic Loading, **Otto Graf Journal**, 6, 47-62.
- CEB (1993) **CEB-FIP Model Code 1990**, CEB Bulletin d'Information No. 213/214, Lausanne.
- Lundgren, K. and Gylltoft, K. (1997) Three-Dimensional Modelling of Bond, in **Advanced Design of Concrete Structures** (eds K. Gylltoft, B. Engström, L-O. Nilsson, N-E. Wiberg, and P. Åhman), CIMNE, Barcelona, 65-72.
- Magnusson, J. (1997) **Bond and Anchorage of Deformed Bars in High-Strength Concrete**. Licentiate Thesis. Division of Concrete Structures, Chalmers University of Technology, Publication 97:1.
- Noghabai, K. (1995) **Splitting of Concrete in the Anchoring Zone of Deformed Bars; A Fracture Mechanics Approach to Bond**. Licentiate Thesis. Division of Structural Engineering, Luleå University of Technology, 1995:26L.
- Tepfers, R. and Olsson, P-Å. (1992) Ring Test for Evaluation of Bond Properties of Reinforcing Bars, in **Bond in Concrete Proceedings** (CEB), Riga, 1-89 - 1-99.
- Åkesson, M. (1993) **Fracture Mechanics Analysis of the Transmission Zone in Prestressed Hollow Core Slabs**. Licentiate Thesis. Division of Concrete Structures, Chalmers University of Technology, Publication 93:5.